

## Original Article

# miR-940 modulates CD47 to suppress biological functions of lung adenocarcinoma cells

Shuzi Long<sup>1\*</sup>, Xizi Long<sup>2\*</sup>, Jing Guo<sup>1</sup>, Liping Fu<sup>3</sup>, Xiaoping Huang<sup>1</sup>, Huawei Liu<sup>1</sup>

<sup>1</sup>Department of Oncology, Chongqing University Three Gorges Hospital, Chongqing University, Chongqing 404100, China; <sup>2</sup>Key Laboratory of Typical Environmental Pollution and Health Hazards of Hunan Province, School of Public Health, Hengyang Medical School, University of South China, Hengyang 421001, Hunan, China; <sup>3</sup>Department of Radiation Oncology, Shanghai East Hospital, Tongji University School of Medicine, Shanghai 200120, China.

\*Equal contributors.

Received September 12, 2023; Accepted March 2, 2024; Epub March 15, 2024; Published March 30, 2024

**Abstract:** Objective: miR-940 and CD47 play regulatory and immunoregulatory roles in lung cancer. While previous study found that the expression of miR-940 decreased, associated with the increasing of CD47 in lung adenocarcinoma. However, their inherent correlations remain elusive. Herein, this experiment intends to search for the relevant molecular mechanisms regulating the biological function of non-small cell lung cancer. Methods: The cancer and adjacent tissue samples were collected from 20 pairs of newly diagnosed non-small cell lung cancer patients without applying radiotherapy and chemotherapy. We performed immunohistochemistry containing 45 lung adenocarcinoma tissues to investigate the relationship between the clinicopathological features and CD47 expression. The expressions of *mir-940* and *CD47* were detected by real-time quantitative polymerase chain reaction (qRT-PCR). Lung epithelial and lung adenocarcinoma (A549, H1299, GLC-82, PC-9) cell lines were cultured to detect the expression of *mir-940* and *CD47* molecules in each cell line. According to the expression situation, 2 cell lines were selected for mimic and siRNA transfection, and the transfection efficiency was also verified by qRT-PCR and western blot. CCK-8, transwell migration, transwell invasion, and colony formation assays were used to detect the changes in biological functions of lung adenocarcinoma cells after transfection, such as enhanced proliferation, migration, invasion, and cloning. The changes of related protein molecules after transfection were detected by western blot. The dual-luciferase experiment verified the targeting regulation relationship between miR-940 and CD47. Finally, flow cytometry analysis of apoptosis and cell cycle were carried out to detect apoptosis cells and change phase of cell cycle distribution. Results: CD47 expression was not associated with clinicopathologic factors in lung adenocarcinoma. The proliferation, migration, invasion, and cloning abilities of lung adenocarcinoma cells were weakened after transfection with miR-940 mimic and siRNA-CD47. Overexpression of CD47 could promote proliferation, migration, invasion, cloning abilities, reduce apoptosis rate and attenuate the antitumor effect of miR-940 on lung adenocarcinoma. Dual luciferase experiments confirmed that miR-940 can target CD47 molecules. Conclusion: miR-940 can inhibit the biological function of lung adenocarcinoma cells by targeting CD47.

**Keywords:** Non-small cell lung cancer, miR-940, CD47, biological function

## Introduction

Lung cancer is one of the most common tumors in the world, the morbidity and mortality continue to increase in recent years up to the top of 23% in men and 22% in women [1]. According to the cancer statistics of the United States in 2020, non-small cell lung cancer (NSCLC) accounts for about 85% of lung cancer. The progression-free survival (PFS) of advanced NSCLC is 4-6 months [2], thereby, most of the lung cancer patients are diagnosed at an

advanced stage and have lost the opportunity for surgery. Given that immunotherapy has lower side effects such as nausea, vomiting, bone marrow suppression, fatigue, anorexia, and hair loss due to the precise targeting and also higher therapeutic effect compared to traditional surgery, radiotherapy, and chemotherapy [3], immunotherapy and targeted cancer therapy have brought a lot of hope to lung cancer patients. For example, the classic immune checkpoint inhibitors including PD-1/L1 blockade and CTLA-4 blockade [4], have been imple-

mented in clinical trials and have shown that they can induce strong anti-tumor effects [4, 5]. CD47, another immune checkpoint, is a protein molecule that is widely expressed on the surface of cell membranes and is related to the immune system. It is also called integrin-associated protein (IAP) which is widely expressed in human normal cells and various tumor cells [6]. One of the functions of CD47 is to protect red blood cells from phagocytosis by macrophages. Also, CD47 is involved in a variety of metabolic pathways in the human metabolism *in vivo*, such as by participating in the thrombospondin-1 (thrombospondin-1) and signal-regulatory protein-alpha (SIRP $\alpha$ ) pathways, affecting cell proliferation, migration, and invasion [7, 8], and send out the “don’t eat me” signal to prevent macrophage-mediated phagocytosis, allowing tumor cells to escape from the recognition of immune cells [9, 10]. Therefore, emerging methods to inhibit the CD47/SIRP $\alpha$  pathway has become prominence for tumor immunotherapy [11].

MicroRNAs are highly conserved noncoding small RNAs with a length of 19-25 nucleotides which are involved in various biological processes of the human body [12]. They can bind to the 3'-Untranslated region (UTR) of target gene mRNAs and affect their protein expression, cell proliferation, migration, invasion, and many other functions [13]. Therefore, the dysregulation of microRNA is closely related to the occurrence and development of many malignant tumors, such as lung cancer, liver cancer, breast cancer, cervical cancer, esophageal cancer, and other tumors [14]. Tan et al. discovered that miR-671-5p can prevent the progression of chemoradiotherapy resistance or drug resistance of breast cancer by targeting the inhibition of FOXM1-gene which mediated epithelial-mesenchymal transition and DNA damage repair [15]. As one kind of microRNA, mir-940 is downregulated in a variety of tumors, suggesting that it acts as a tumor suppressor gene. Wang et al. demonstrated that the expression of mir-940 which regulates the PKC- $\delta$  gene is decreased in ovarian cancer, by increasing the expression of mir-940 to inhibit the proliferation of ovarian cancer cells and inducing their apoptosis [16]. Jiang et al. reported that mir-940 inhibits epithelial-mesenchymal transition and invasion of NSCLC by targeting the snail gene [17]. Accordingly, mir-940 may

be involved in the occurrence and development of tumors as a tumor suppressor gene in non-small, whereas, in the field of NSCLC, no targets have been found for mir-940. In this study, we identified that mir-940 is associated with CD47 by bioinformatics analysis. Then, the expression of mir-940 and CD47 in lung cancer cells were intervened here to explore the relationship between mir-940 and CD47 including their binding positions, possible signaling molecular pathway, and biological function.

## Materials and methods

### Tissue specimens

We collected 20 non-small cell lung cancer tissues including cancer tissues and normal tissues (5 cm away from the carcinoma region). Tissues were frozen in liquid nitrogen immediately and placed in the -80°C refrigerator for further experiments. All the patients are from the Department of Thoracic Surgery of Chongqing University Three Gorges Hospital from August 2020 to October 2020. The patients were newly diagnosed with non-small cell lung cancer without radiotherapy and chemotherapy treatment. All the assays have obtained the informed consent of the patients and their families and have been approved by the ethics committee of Chongqing University Three Gorges Hospital.

### MiRNA microarrays and miRNA target prediction

Total RNA was extracted from 10 pairs of lung cancer tissues and normal tissues with TRizol (Takara, Japan). The PCR products were further purified (AMPure XP system) and then the library quality was assessed. Index-encoded samples were clustered on the cBot Cluster Generation System using the TruSeq PE Cluster Kit v4-cBot-HS (Illumia). Based on a volcano plot and fold-change filtering, we identified the differentially expressed miRNAs in non-small cell lung cancer. Candidate miRNAs were included by the following criteria: (1) *P* values were less than 0.05; (2)  $|\log_2 \text{FC}| > 1$ . Target gene function annotation and gene functions were annotated based on the following databases: Swiss-Prot (manually annotated and reviewed Protein Sequence Database); KEGG (KEGG Ortholog Database); GO (Gene Onto-

logy). GO enrichment analysis and KEGG pathway enrichment analysis were used to analyze the pathways of the differential miRNAs. TargetScan was used to forecast the target genes of miRNAs and possibly potential binding sites.

### Cell culture

Human lung epithelial cells (HBE) were purchased from Promega Company. A549, H1299, and PC-9 were purchased from Bopei Company. BLC-82 cells were preserved by the Central Laboratory of the Chongqing University Three Gorges Hospital. The cells were cultured in RPMI1640 medium containing 10% fetal bovine serum, placed in a 37°C, 5% CO<sub>2</sub> cell incubator, passaged and frozen when the cells were in the logarithmic phase. Cells were digested with 0.25% trypsin (EDTA, phenol red) at passage. The new Saimei serum-free cryopreservation solution was used to freeze the cells in a -80°C refrigerator for a long time.

### Tissue and cell RNA extraction and qRT-PCR

RNAiso Plus (Takara Japan) were used to extract total RNA from lung cancer tissues and lung cancer cells, and the extracted RNA was stored at -80°C refrigerator. The All-in-One™ miRNA qRT-PCR Detection System was used to synthesize the first-strand cDNA of lung cancer tissue and lung cancer cells respectively. Then the Realtime PCR application (Analytik Jena, Germany, qTOWER2.2) was used for qPCR analysis, also U6 was used as an internal reference. The cDNA was synthesized by reverse transcription using SureScript™ First-Strand cDNA Synthesis Kit, and the Realtime PCR application (Analytik Jena, Germany, qTOWER2.2) was also used for qPCR analysis, and ACTB was used as an internal reference. The result is calculated using 2 -ΔΔct.

### Cell transfection and verification

The A549 and H1299 cells were plated into six-well plates at a desity of 50 × 10<sup>4</sup> respectively. When the cell confuence was about 60%, H1299 cells were transiently transfected with CD47 siRNA (CD47-homo-228 CD47-homo-649) and si-NC, CD47 overexpression plasmid pcDNA3.1-CD47 (CD47) and empty pcDNA3.1 plasmid (Vector) (GenePharma, Shanghai, China) using Lipofectamine 2000 (Invitrogen, USA) following the instructions.

Then A549 and H1299 cells were transiently transfected with negative control (NC) and mir-940 mimic (GenePharma, Shanghai, China) using Lipofectamine 2000 (Invitrogen, USA) following the instructions. Finally negative control (NC) + empty pcDNA3.1 plasmid (Vector), mir-940 mimic (mir-940) + empty pcDNA3.1 plasmid (Vector), mir-940 mimic (mir-940) + over-expression plasmid pcDNA3.1-CD47 (CD47) were co-transfected into A549 cells transiently also using Lipofectamine 2000 (Invitrogen, USA) reagents.

The sequences of various small RNAs are as follows: mir-940 mimic (5'-AAGGCAGGGCCCC-CGCUCCCC-3'); mir-NC/si-NC (5'-UUCUCCGAA-CGUGUCACGUUTT-3'); CD47-homo-228 (5'-CAG-CUCAGCUACUAUUUAATT-3'); CD47-homo-649 (5'-GGGACAGUUUGGUAUUAAATT-3').

After the above-mentioned procedures, the trasfection efficiency verified by qRT-PCR and western blot after transfection for 48 hours.

### Cell proliferation assay

The varied proliferation abilities of A549 and H1299 cells after transfection were detected by CCK-8 kit respectively. Firstly, the transfected A549 and H1299 cells were seeded in 96-well plates (3 × 10<sup>3</sup> cells/well), and the cells were cultured at 37°C, and a 5% CO<sub>2</sub> humidified atmosphere. 10 μL of CCK-8 reagent was added to each well. Then Spectra Max M4 (Molecular De vices, USA) was used to detect 450 nm optical density (OD) at 0 h, 24 h, 48 h, and 72 h, finally, we used GraphPad Prism 5 to draw the cell proliferation curve.

### Cell migration and invasion assay

The transfected A549 and H1299 cells resuspended in serum-free medium were added into the upper chamber at 3 × 10<sup>4</sup>/200 μL, and 700 μL 10% fetal bovine serum was added to the lower chamber, the cells were cultured in a 37°C, 5% CO<sub>2</sub> humidified atmosphere for 20 hours, next wash the chamber with phosphate-buffered saline (PBS), and then fix the crossed cells with 4% paraformaldehyde (PFA, Servicebio, Wuhan, China) at room temperature, and finally cells were stained with 1% crystal violet (crystal violet, Solarbio, China). Three random fields of view were selected under the microscope for photographing and cell count-

ing (LeicaMicrosystem LASV4.9, Germany). The steps of the invasion experiment are the same as those of the migration experiment, the difference is that Matrigel base glue is added in the upper chamber of the invasion experiment.

### *Cell colony formation experiment*

The transfected A549 and H1299 cells ( $8 \times 10^2$  cells/well) were seeded into six-well plates, and after 7 days' culture, the cells were fixed with 4% paraformaldehyde (PFA, Servicebio, Wuhan, China), and then washed twice with phosphate-buffered saline (PBS), finally stained with 1% concentration of crystal violet (crystal violet, Solarbio, China) for 30 minutes.

### *Dual luciferase assay*

The interaction sites between mir-940 and CD47 were predicted by bioinformatics software (TargetScanHuman), then, the sequences of CD47 MUT-hsa-miR-940 and CD47 WT-hsa-miR-940 were synthesized and cloned into GP-miRGLO vector. In A549 and H1299 cells, the constructed vector was co-transfected with mir-940 mimic and NC using GP-transfect-Mate (Zima Gene, Shanghai), and divided into mimic NC + CD47 homo WT; has-mir-940 mimics + CD47 homo WT; mimic NC + CD47 homo MUT; has-mir-940 mimics + CD47 homo MUT four groups, the cells were collected at 48 h after transfection, and the Dual-Luciferase reporter gene detection system kit (GenePharma) was used, then the luciferase activity was detected using Synergy HTX microplate reader (Biotek).

### *Flow cytometry analysis of apoptosis*

After transfection, the A549 and H1299 cells were seeded in 6-well plates. The cells were collected by trypsin and washed with 5 ml phosphate-buffered saline (PBS), then suspended with 100  $\mu$ L binding buffer. The mixed liquid was incubated in the dark place after adding 5  $\mu$ L Annexin V-FITC and 5  $\mu$ L propodium iodide (PI). Finally, the apoptotic cells were detected with flow cytometry.

### *Flow cytometry analysis of cell cycle*

The transfected cells were collected by centrifuge with 12000 rpm, then washed twice with 5 mL phosphate-buffered saline (PBS), later added 3 ml cold alcohol in the suspension at

4°C temperature for 24 hours. The cells washed with PBS twice again, added 2.5  $\mu$ L DNA enzyme inhibitor and 5  $\mu$ L propodium iodide (PI) incubated in the dark for 30 minutes. Finally, the cell samples were detected by flow cytometry.

### *Protein extraction and western blot experiments*

After transfection, we extracted proteins with Protein Extraction Kit (BC3710, Solarbio), measured the protein concentration with a BCA protein concentration assay kit (Biyuntian, China), added 1/4 total volume of SDS-PAGE protein loading buffer (5 $\times$ ), and then boiled protein at 100°C for 5 min. 40  $\mu$ g protein samples were separated on 10% SDS-PAGE gels and then electroblotted onto polyvinylidene fluoride (PVDF) membranes of the corresponding size, which electro-transferred at 0°C and 250 mA. The membrane was blocked with 50 g/L nonfat milk at room temperature for 2 h, washed with TBST, the PVDF membranes were incubated with the following primary antibodies: Mouse anti-human p-AKT (1:1000), p-PI3K (1:1000), p-mTOR (1:1000), GAPDH (1:300), and incubated on a freezer shaker overnight (at least 8 hours) at 4°C, subsequently the PVDF membranes were washed three times with TBST. After washing, the secondary antibody HRP rabbit anti-mouse IgG (1:3000) was incubated on the PVDF membrane at room temperature for 2 hours and then washed three times with TBST for 10 min each time. Finally, ECL chemiluminescence reagent, A solution:B solution = 1:1 (Biyuntian, China) was used for imaging, and a dual-color infrared fluorescence imaging system (Analytik Jena, Germany) was used for exposure. Image J was used for gray value analysis of protein bands and cell counting.

### *Immunohistochemical staining and immunohistochemical analysis of CD47*

We collect 45 paraffin-embedded (FFPE) sections from the patients who were newly diagnosed with lung adenocarcinoma between 2019 to 2022, then we used the AutostainerLink 48 automated staining system (Dako Autostainer Link 48 instrument, Denmark) to perform the immunohistochemical staining of CD47 with 4- $\mu$ m-thick sections after that Anti-CD47 rabbit monoclonal antibody were used (with dilution factor of 1:100) to perform Im-

**Table 1.** Baseline characteristics of lung adenocarcinoma patients

Factors	Value
Number of patients	45 (100%)
T stage	
1&2	34 (75.6%)
3&4	11 (24.4%)
N stage	
0	21 (46.7%)
1&2&3	24 (53.3%)
M stage	
0	16 (35.6%)
1	29 (64.4%)
TNM stage	
I&II	8 (17.8%)
III	8 (17.8%)
IV	29 (64.4%)
Gender	
Male	22 (48.9%)
Female	23 (51.1%)
Age	
< 60 years	22 (48.9%)
≥ 60 years	23 (51.1%)
Smoke	
Yes	23 (51.1%)
No	22 (48.9%)
Mutation	
ALK	7 (15.6%)
EGFR	25 (55.6%)

munohistochemical studies. Two experienced pathologists independently evaluated the hematoxylin and eosin (H&E)-stained slides and records the clinicopathological characteristics. The expression of CD47 depends on the staining intensity and staining ratio, we score the stained slides into four levels (negative for 0, weak for 1+, moderate for 2+, strong for 3+). Sample scored 1+, 2+, and 3+ was regarded as CD47 positive expression.

#### Statistical analysis

SPSS 22.0 statistical software, Graphpad Prism5 was used to draw graphs, ImageJ software was used to analyze gray value of western blot assay and the cell counts of transwell experiment, and the data were expressed as means ± standard deviation (SD). Differences between two groups were analyzed by two-tailed unpaired Student's test, and differences among more than two groups were analyzed by

one-way ANOVA. The  $\chi^2$  test was used to evaluate the association between CD47 expression and clinicopathological factors. A p-value less than 0.05 was considered statistically significant. \* $P < 0.05$ , \*\* $P < 0.01$  and \*\*\* $P < 0.001$ .

## Results

*Identifying differential microRNA and correlated target sequence, miR-940 was down-regulated in NSCLC, while CD47 was up-regulated*

To verify the impact of microRNA to signal pathways for occurrence and development in NSCLC cells, 10 pairs of lung cancer tissue samples were collected and sequenced by the microRNA high throughput platform. It was observed that 361 miRNAs expression up-regulated and 276 of that decreased, which is corresponding to the GO clustering results of target genes of differential microRNAs: significant clustering alterations in the biological processes of the immune system process, biological adhesion, and cell response stimulation were observed, suggesting that the genes related to immune microenvironment are significantly regulated after tumorigenesis (Figure S1). Further assessment by KEGG signal pathway enrichment analysis of differential miRNA target genes revealed that differential miRNA target genes were significantly enriched in the tight junction signal pathway, cell adhesion molecules signal pathway, and endocytosis signal pathway (Figure S1).

In-depth data mining of sequencing results through Software Miranda and Targetscan further noticed that the gene of CD47/CDH15/MAGI2/PARD3 and their correlated microRNA genes hsa-miR-940/hsa-miR-9901/hsa-miR-7704/hsa-miR-23a-5p/hsa-miR-671-5p would be critical in NSCLC (Table 1). Among them, the expression of hsa-mir-9901, hsa-mir-7704, and hsa-mir-671-5p were significantly up-regulated in tumor tissues, while the expression of hsa-mir-940 and hsa-mir-23a-5p were down-regulated in tumor tissues. Further assessment by the qRT-PCR confirmed that the expression levels of these microRNAs were different in tumor tissues (Figure 1A), which is associated with the regulation of downstream target genes (Figure 1B) obviously.

#### CD47 expression in clinicopathologic features

Based on the characteristics of lung adenocarcinoma patients in Table 1, we have defined

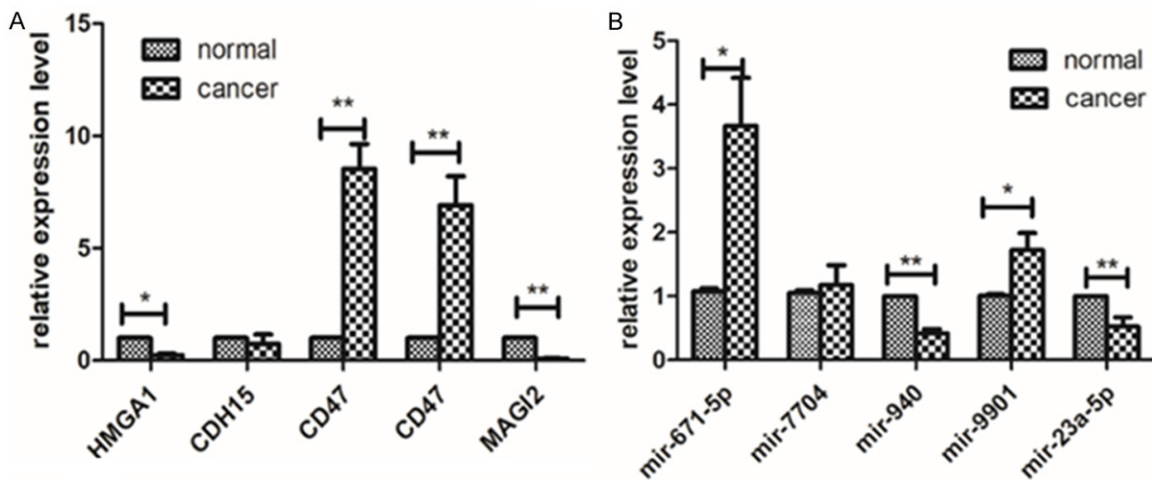


**Figure 1.** Differential expression of genes between NSCLC tissues and normal controls. A. The potential target genes (HMGA1, CDH15, CD47, CD47, MAGI2) in NSCLC tissues and normal tissues. B. The relative expression of miRNAs (hsa-mir-671-5p, hsa-mir-7704, mir-940, hsa-mir-9901, hsa-mir-23a-5p).

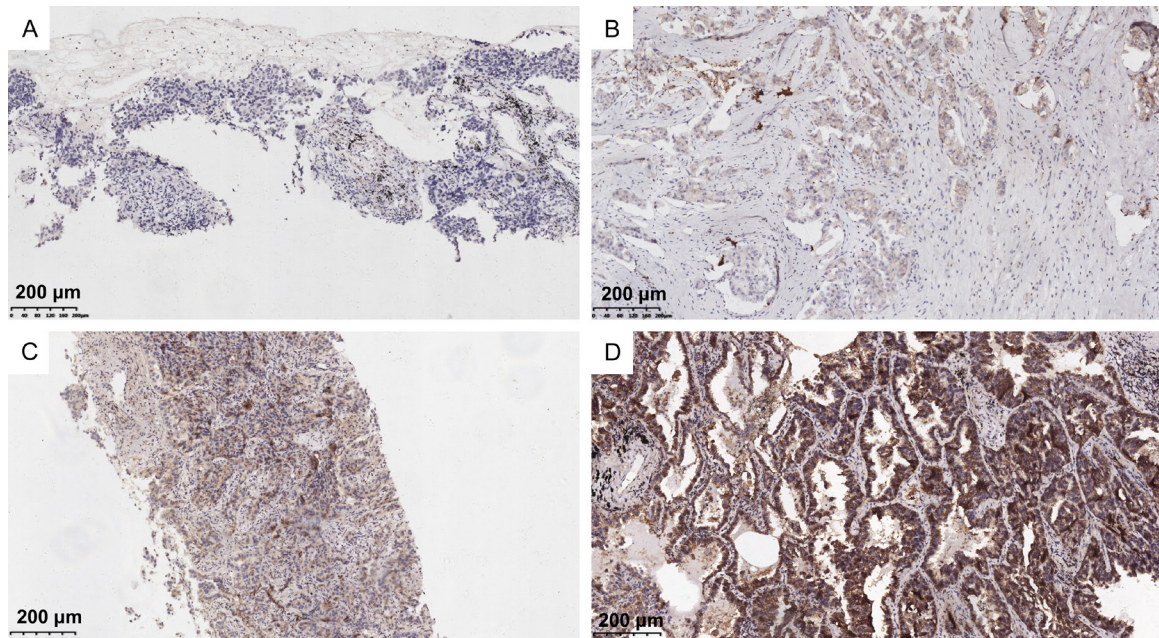


**Figure 2.** CD47 expression in lung adenocarcinoma tissues. According to the dyeing strength (A) graded as negative (0). (B) is graded as weak (1+). (C) was graded as moderate (2+). (D) was graded as strong (3+). (B-D) were all positive. Bar = 200  $\mu$ m.

“0” as negative, and “1+, 2+, 3+” as positive of the featured 45 lung adenocarcinoma patients (**Figure 2**). 75.6% of patients were classified as T1&T2, 24.4% of patients were T3&T4, and 46.7% of patients had no regional lymph node metastasis, while 53.3% of patients had lymph node metastasis. Most of the patients have distant metastasis at the time of diagnosis (64.4%), and there were 8 (17.8%) stage I-II

patients, 8 (17.8%) stage III patients, and 29 (64.4%) stage IV patients. 22 (48.9%) of them were male, and 23 (51.1%) of them were smokers. As for ages, 23 (51.1%) of them exceeded 60 years old. Only 7 (15.6%) of them had ALK gene mutation, and 25 (55.6%) patients had EGFR gene mutation. **Table 2** shows the relationship between CD47 expression and clinicopathologic factors: the T, N, M, stage, smoke,

**Table 2.** Correlation between CD47 expression and clinicopathologic factors in lung adenocarcinoma

Clinicopathologic Factors	n	CD47 Expression		P Value
		Negative (%)	Positive (%)	
T				0.54
T1&T2	34	10 (29.4%)	24 (45.5%)	
T3&T4	11	5 (70.5%)	6 (54.5%)	
N				0.75
N0	21	8 (38.1%)	13 (61.9%)	
≥N1	24	7 (29.2%)	17 (70.8%)	
M				0.58
M0	16	4 (25%)	12 (75%)	
M1	29	11 (37.9%)	18 (62.1%)	
Stage				0.73
I&II	8	2 (25%)	6 (75%)	
III	8	2 (25%)	6 (75%)	
IV	29	11 (37.9%)	18 (62.1%)	
Smoke				1
Yes	23	8 (34.8%)	15 (65.2%)	
No	22	7 (31.8%)	15 (68.2%)	
Mutation				0.22
ALK	7	1 (14.3%)	6 (85.7%)	
EGFR	25	11 (44%)	14 (56%)	
Gender				0.9
Male	22	8 (36.4%)	14 (63.6%)	
Female	23	7 (30.4%)	16 (69.5%)	
Age				0.46
≥60	22	9 (40.9%)	13 (59.1%)	
<60	23	6 (26.1%)	17 (73.9%)	

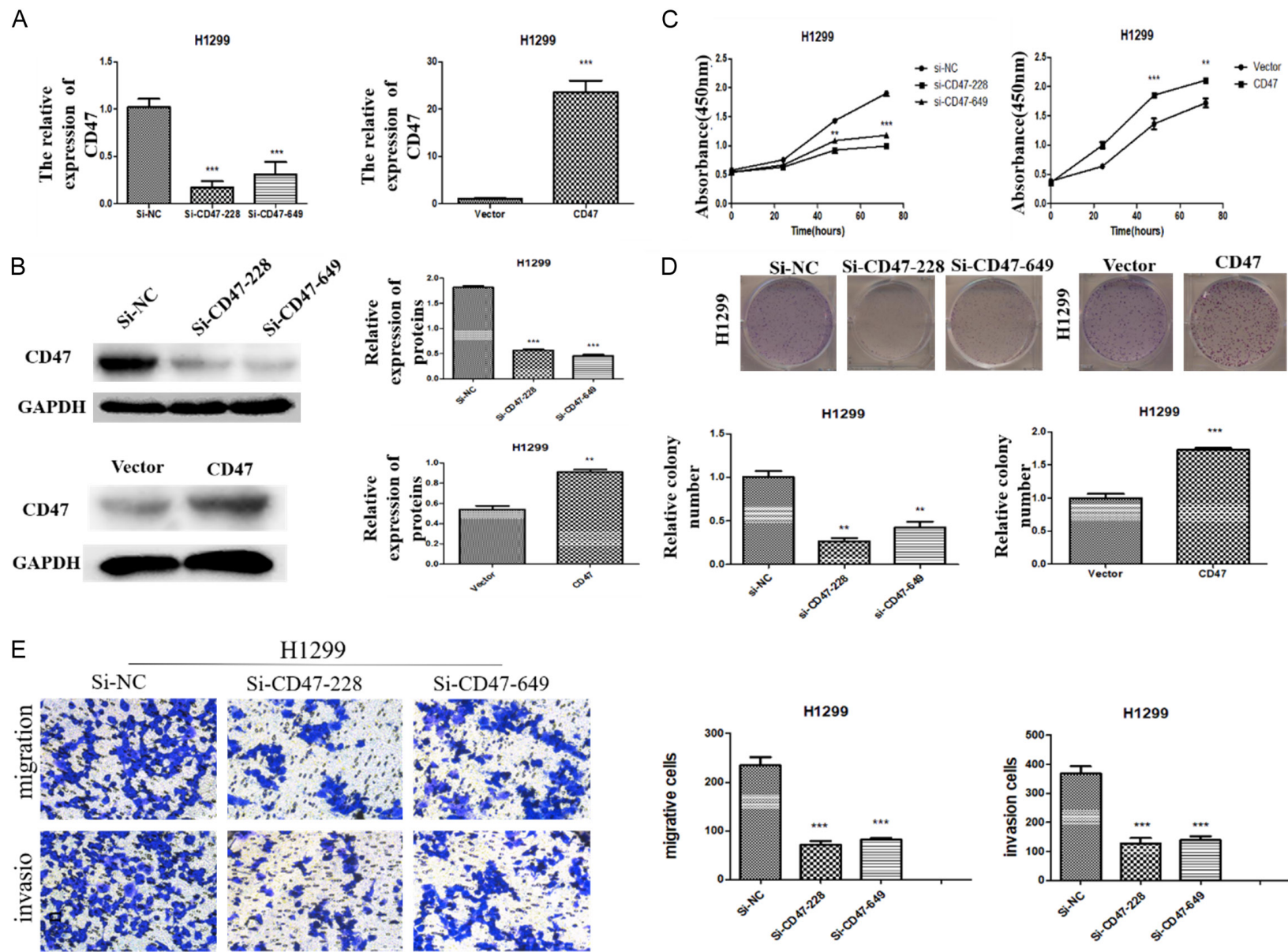
mutation of ALK and EGFR, gender, and age were not associated with CD47 expression ( $P > 0.05$ ).

*Reducing the expression of CD47 inhibits the proliferation, migration, invasion and promotes apoptosis of lung adenocarcinoma cells, while upregulating the expression of CD47 has an opposite results*

It's evident that CD47 remarkably influence the biological effects on NSCLC cells, and we down-regulating the expression of CD47 to further confirm the results. The transfection efficiency was detected by qRT-PCR and western blot. The outcomes of qRT-PCR showed that the expression of CD47 in the Si-CD47-228, Si-CD47-649 groups were significantly lower than that in the Si-NC group after transfection with Si-CD47. While the CD47 expression in CD47 group was much higher than in the vector group

( $P > 0.05$ ), the western blot assay shows the same results, so the transfections were succeeded (Figure 3A, 3B). The CCK-8 assays were conducted to detect the changes in the proliferation ability of the cells after transfection. As shown in Figure 3C, the OD<sub>450</sub> value of the experimental group was significantly lower than that of the negative control group, indicating that the proliferation ability would be inhibited after transfection with Si-CD47. While, the proliferation ability was increased by up-regulating the expression of CD47 (Figure 3C). The colony formation assays show the same results of variable proliferation ability on NSCLC cells, the colonies were significantly decreased in the Si-CD47-228, Si-CD47-649 group but increased in the CD47 group (Figure 3D). The effect of CD47 on migration and invasion abilities was measured by transwell assay. The results showed that migrative and invasive capabilities were weakened in the Si-CD47 group, however

# miR-940 suppress biological functions of lung adenocarcinoma cell



## miR-940 suppress biological functions of lung adenocarcinoma cell

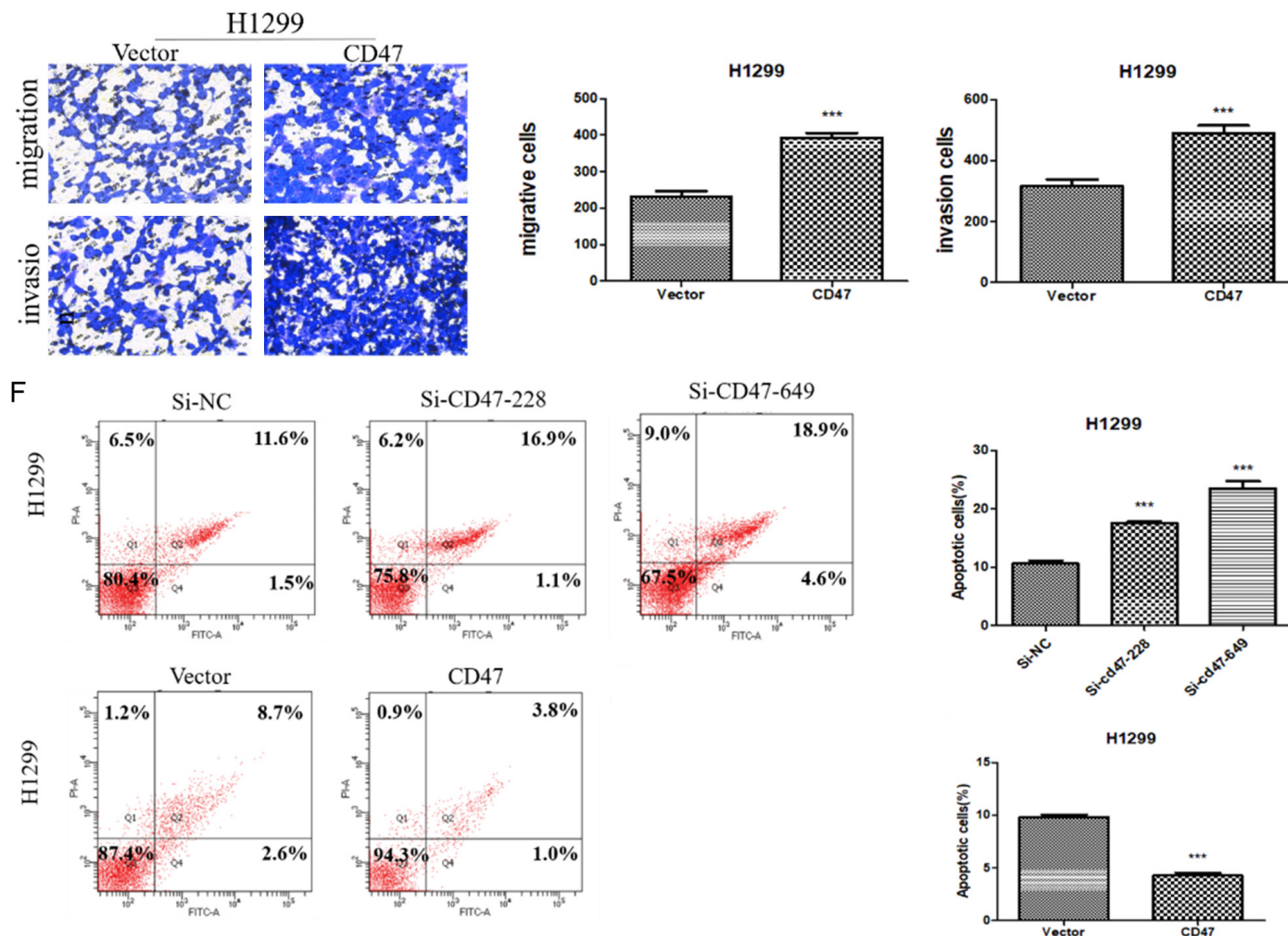


**Figure 3.** The overexpression of CD47 promotes proliferation, migration, invasion and apoptosis ability. A. After transfection, the relative expression of CD47 were detected by qRT-PCR. B. The relative expression of proteins were analyzed by western blot after transfection in H1299. C, D. The CCK-8 assay and colony formation assay were used to examine the varible proliferation ability. E. The migrative and invasive capacity of H1299 were detected by transwell migration and invasion assays. F. Flow cytometry analysis of apoptosis show the cell apoptosis rate (Q2+Q4) in H1299 cells after transfection.

strengthened in the CD47 group (**Figure 3E**). To further investigate the function of CD47 on apoptosis, the flow cytometry analysis of apoptosis indicates that down-regulating the expression of CD47 promoted NSCLC cell apoptosis, while overexpression of CD47 restrain the apoptosis (**Figure 3F**).

*Up-regulating miR-940 inhibits the proliferation, migration, and invasion of human lung epithelial cells*

We transfected the miR-940 mimic into NSCLC cells H1299 and A549 by lipo3000 and tested the transfection efficiency by qRT-PCR. It was found that the expression of miR-940 after transfection was significantly higher than that of the negative control (NC) group, suggesting that transfection was successful (**Figure 4A**). Then, the CCK-8 experiments were conducted to verify the change of cell proliferation ability after transfection of miR-940 mimic. As shown in **Figure 4B**, the absorbance (OD = 450 nm) values of H1299 and A549 at 24 h, 48 h, and 72 h after transfection of the miR-940 mimic were remarkably lower than the control (**Figure 4B**). Meanwhile, we can see that the number of transmembrane cells in the experimental group was lower than that in the NC group after H1299 and A549 cells were transfected with miR-940 mimic (**Figure 4C, 4D**). Also in the invasion experiment, it was observed that after transfection of miR-940 mimic, the number of cells in the experimental group of H1299 and A549 cells is also smaller compared with the NC group (**Figure 4E, 4F**). To understand the effect of miR-940 on the cloning ability of lung adenocarcinoma cells, we used the clone formation assay to detect the changes in the colony formation ability of H1299 and A549 cells. The experimental results indicated that the number of colonies in the experimental group was significantly smaller than that in the NC control group (**Figure 4G, 4H**). Western-blot experiments showed that after transfection of miR-940 mimic, the expression of AKT, PI3K, and mTOR protein molecules decreased, suggesting that miR-940 may inhibit the biological behavior of lung adenocarcinoma cells by inhibiting the activation of AKT/PI3K pathway (**Figure 4I, 4J**). Generally, the experiments confirmed that increasing the expression of miR-940 could further inhibit the proliferation, migration, inva-

sion, and colony formation ability of lung adenocarcinoma cells.

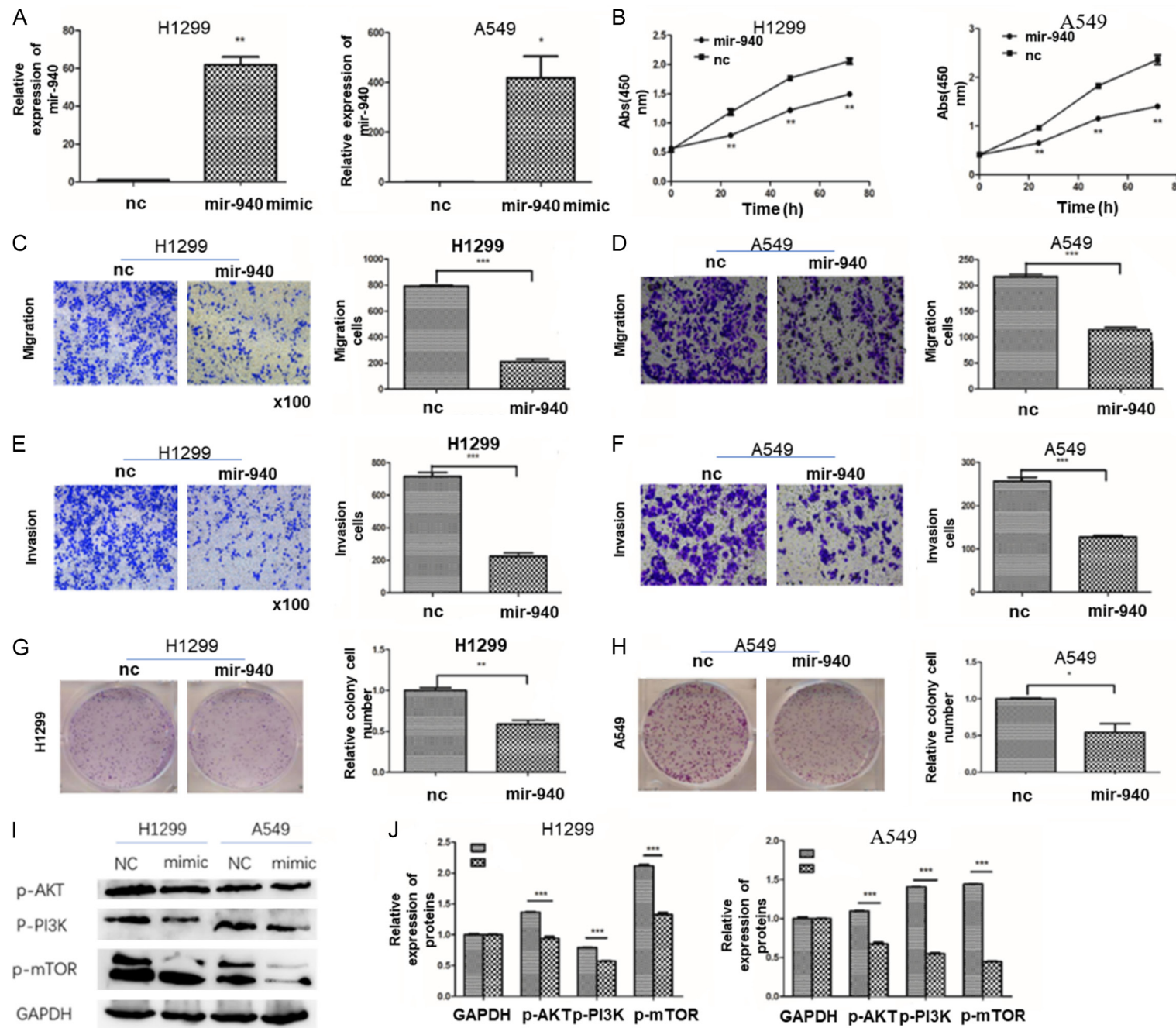
*CD47 is a direct target of miR-940*

Based on the bioinformatical analysis, it has been speculated that miR-940 inhibits the biological function of lung adenocarcinoma cells by targeting CD47 at two binding sites as shown in **Figure 5A**. Hence, dual luciferase experiments were conducted here to verify the targeting relationship. First, we cloned the constructed CD47 WT-hsa-miR-940 and CD47 MUT-hsa-miR-940 sequences into the GP-miRGLO vector, and then transfected with NC and miR-940 mimic into A549 and H1299 cells respectively, the results showed that the ratio of firefly luciferase/Renilla luciferase in the miR-940 mimic group was significantly lower than that in control NC group both in H1299 and A549 cells, suggesting that miR-940 can inhibit CD47 expression by targeting the 3'-UTR region (**Figure 5B, 5C**), thereafter affecting the expression of downstream signaling pathway molecules. Meanwhile, since the expression of miR-940 was decreased in lung cancer tissues by qPCR, while the expression of CD47 was significantly increased (**Figure 5D, 5E**), an inverse correlation between miR-940 and CD47 was also simply confirmed in 20 NSCLC samples (Pearson correlation = -0.826,  $P < 0.001$ ; **Figure 5F**).

*Overexpression of CD47 attenuated the inhibitory effect of miR-940 in NSCLC*

To further prove that miR-940 inhibits the proliferation, migration, invasion ability of NSCLC cells by targeting CD47, we transfected A549 cells with the following co-transfection materials: negative control (NC) + empty pcDNA3.1 plasmid (Vector), miR-940 + empty pcDNA3.1 plasmid (Vector), and miR-940 + pcDNA3.1-CD47 plasmid (CD47). The transfection efficiency was assessed using qRT-PCR and western blot. Notably, the expression of CD47 in the miR-940 + Vector group was lower than that in the miR-940 + CD47 group (**Figure 6A, 6B**). Subsequent experiments were conducted to confirm that CD47 could mitigate the inhibitory effect of miR-940 on itself. The proliferation capability was notably enhanced in the miR-940 + CD47 group compared to the miR-940 + Vector group (**Figure 6C**).

## miR-940 suppress biological functions of lung adenocarcinoma cell



## miR-940 suppress biological functions of lung adenocarcinoma cell

**Figure 4.** Biological function analysis of miR-940. (A) After transfection, the relative expression of miR-940 was detected by qRT-PCR. (B) CCK-8 assays show the variable proliferation of H1299 and A549 cells after transfection with miR-940 mimic and NC. (C-F) The migration, and invasion assays show the cell count of H1299 and A549 cells after transfection with miR-940 mimic and NC. (G, H) Colony formation assay indicating clone formation ability of H1299 and A549 cells. (I, J) The relative expression of proteins (p-AKT, p-PI3K, and p-mTOR) were detected by western blot. Bar = 100  $\mu$ m (C, E), 200  $\mu$ m (D, F).

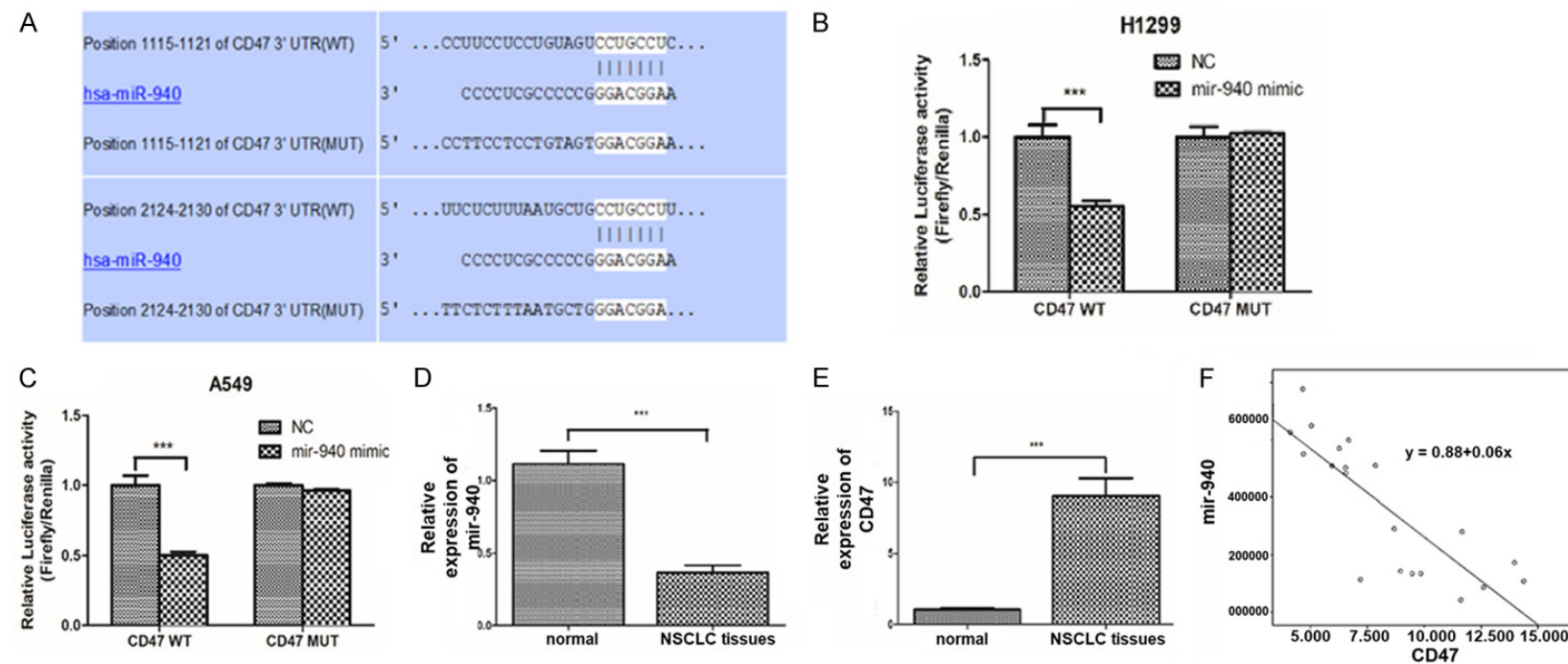
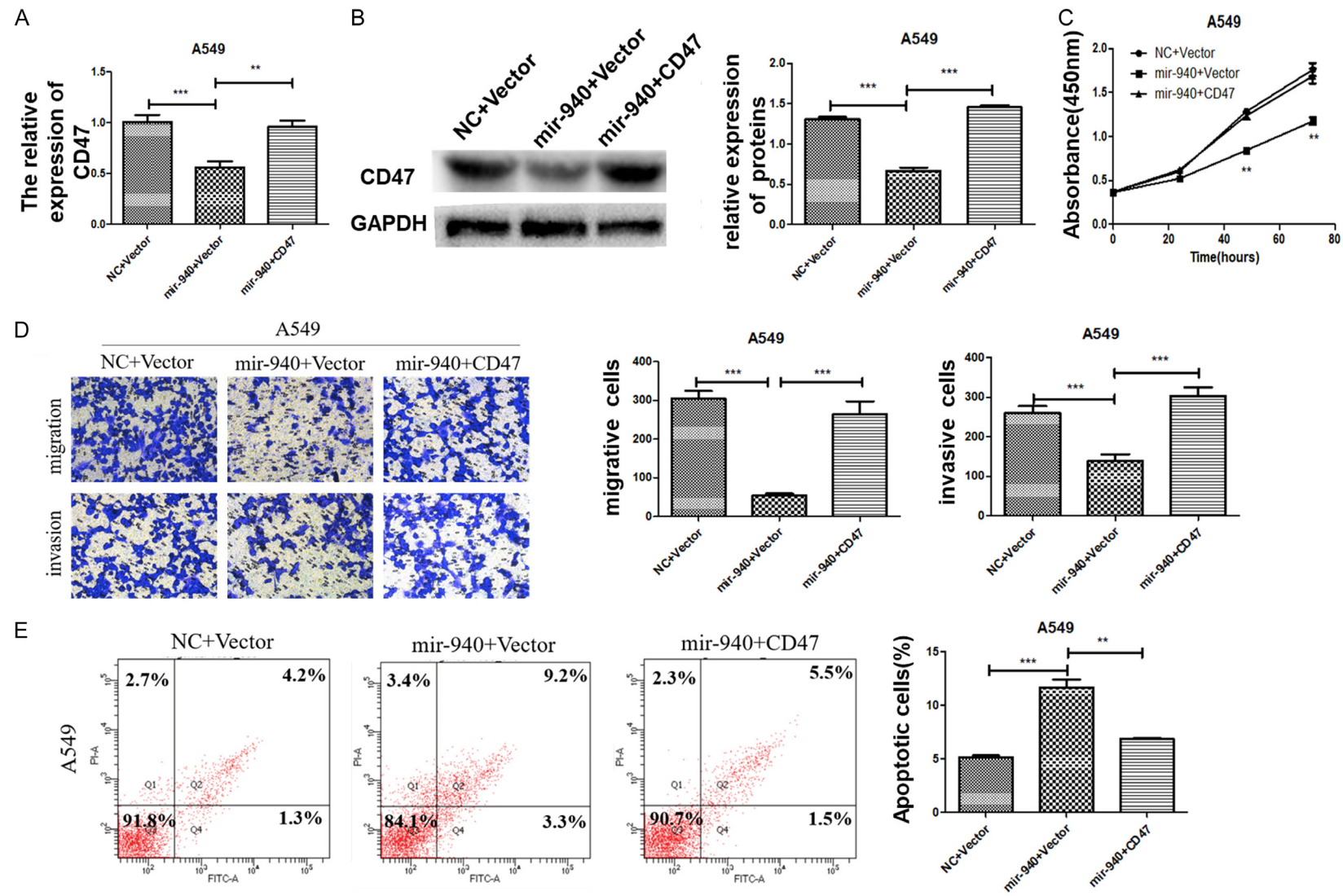


**Figure 5.** miR-940 directly targeting CD47. A. The potential binding sites between miR-940 and CD47. B, C. Luciferase activity detection in H1299 and A549 cells co-transfected with miR-940 mimic and CD47 3'UTR-wild/mutant-type reporter plasmids. D, E. The relative expression of miR-940 and CD47 between NSCLC tissues and normal tissues. F. A Pearson correlation analysis of CD47 and miR-940.

# miR-940 suppress biological functions of lung adenocarcinoma cell



## miR-940 suppress biological functions of lung adenocarcinoma cell

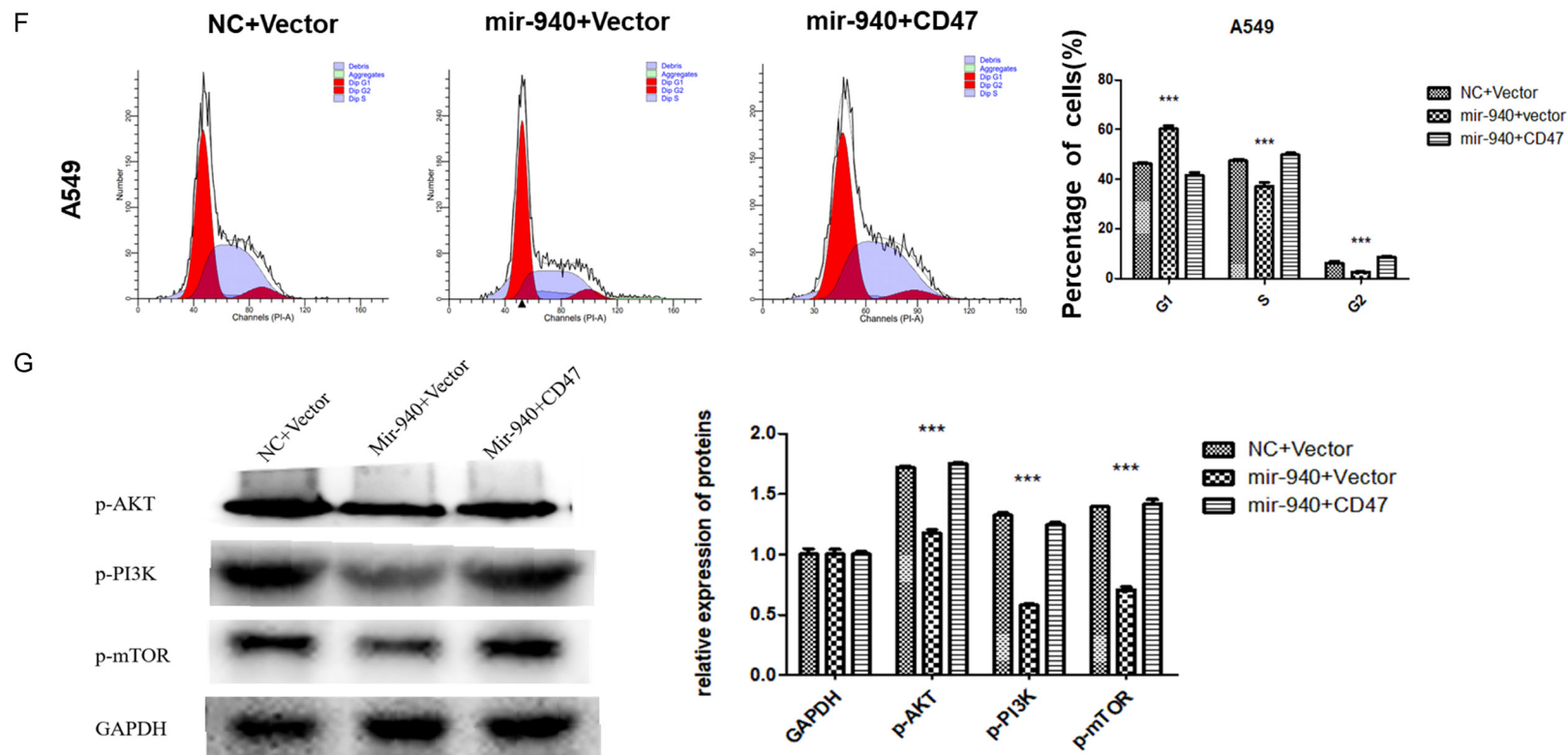


**Figure 6.** Overexpression of CD47 attenuates the effect of miR-940 on proliferation, invasion, and apoptosis. A. CD47 expression was detected by qRT-PCR after A549 cells were transfected with miR-940 mimics and CD47 overexpression plasmids. B. The transfection efficiency was verified by western blot. C. CCK-8 assay was used to detect the proliferation ability. D. Transwell assays were conducted to detect the migration and invasion ability of A549 cells. E. Up-regulation of CD47 reduces the effect of miR-940 on apoptosis. F. Cell cycle assays were conducted in A549 cells after transfection. G. The relative expression of p-AKT, p-PI3K, and p-mTOR proteins were detected by western blot.

Our study further revealed increased migration and invasion abilities in the miR-940 + CD47 group (**Figure 6D**). And the apoptosis rate was higher in the miR-940 + Vector group compared to the miR-940 + CD47 group (**Figure 6E**). The cell cycle experiment demonstrated that G1 phase arrest was alleviated in the miR-940 + CD47 group compared to the miR-940 + Vector group (**Figure 6F**). Additionally, the expression levels of p-AKT, p-PI3K, and p-mTOR proteins were lower in the miR-940 + Vector group compared to the miR-940 + CD47 group (**Figure 6G**). In summary, these findings indicate that CD47 can attenuate the suppressive effect of miR-940 on A549 cells. Furthermore, these results provide additional confirmation that CD47 is a direct target of miR-940.

## Discussion

The miR-940 gene is located on chromosome 16P13.3 and can bind to the 3'UTR region of target genes, inhibiting the transcription and post-transcriptional regulation of protein-coding genes [18]. Furthermore, miR-940 is found to be dysregulated in various malignant tumors, including breast cancer, liver cancer, non-small cell lung cancer, ovarian cancer, and others. It plays a crucial role in several cellular biological processes, such as cell proliferation, migration, invasion, apoptosis, and epithelial-mesenchymal transition [18]. In our research, we conducted gene sequencing of NSCLC tissues and identified several differentially expressed microRNAs, including miR-940, hsa-mir-9901, hsa-miR-7704, hsa-miR-23a-5p, and hsa-miR-671-5p. We also discovered potential target molecules: CD47, CDH15, MAGI2, and PARD3.

Our study revealed a decreased expression of miR-940 in lung adenocarcinoma cells and lung cancer tissues, indicating its potential role as a tumor suppressor gene involved in various aspects of lung cancer. For instance, Xu et al. reported that miR-940 inhibited epithelial-mesenchymal transition by targeting the ZEB2 gene in glioma cells [19], while Luo et al. demonstrated its effects on proliferation and cell cycle regulation in glioma by targeting the CKS1 gene [20]. Subsequently, we confirmed the reduced expression of miR-940 in lung cancer cells using qPCR, and its biological function was verified through CCK-8, transwell, and colony formation experiments. Following transfection, we observed reduced proliferation, migration,

invasion, and clone formation abilities of H1299 and A549 cells. Thus, our research establishes miR-940 as an important player in the occurrence and development of lung adenocarcinoma as a tumor suppressor gene.

CD47 is an integrin protein acting as an immune-related regulator, widely expressed in both normal cells and various tumor cells, such as red blood cells, ovarian cancer, breast cancer, colon cancer, bladder cancer, glioblastoma, hepatocellular carcinoma, prostate cancer, and lung cancer. It plays a role in negatively regulating macrophages by binding to the signal transduction protein alpha (SIRP $\alpha$ ) on the macrophage membrane [21, 22]. CD47 inhibits macrophage phagocytosis of tumor cells by interacting with SIRP $\alpha$  molecules on the macrophage membrane [9, 10]. Recent studies have demonstrated that blocking CD47 expression on tumor cells can enhance antibody-dependent phagocytosis. As a result, specific CD47-blocking antibodies have been reported to inhibit the binding of CD47 to SIRP $\alpha$  on macrophage membranes, thus enhancing macrophage-mediated phagocytosis of tumor cells [23]. However, some studies have associated CD47 overexpression with certain clinicopathological factors and a poor prognosis [24, 25]. Despite this, an Immunohistochemistry experiment did not reveal a correlation between CD47 expression and clinicopathological features, highlighting the importance of expanding the sample size to reach more definitive conclusions.

Furthermore, our research found significantly higher CD47 expression in lung cancer tissue specimens and lung adenocarcinoma cells compared to normal tissues and Human bronchial epithelial cells (HBE). By reducing CD47 expression, we observed inhibited proliferation, migration, and invasion abilities of lung adenocarcinoma cells, consistent with the upregulation of miR-940 expression. Pearson correlation analysis confirmed an inverse relationship between miR-940 and CD47. Subsequent target gene prediction and dual luciferase experiments validated that miR-940 can target and regulate CD47 expression in lung adenocarcinoma cells. These findings suggest that miR-940 may enhance macrophages' ability to recognize and eliminate tumor cells by preventing the CD47/SIRP $\alpha$  axis. In our investigation, we demonstrated that CD47 serves as a direct tar-

get of miR-940. The overexpression of CD47 was found to enhance proliferation, migration, and invasion capabilities, while simultaneously reducing apoptosis and counteracting the inhibitory impact of miR-940 on lung adenocarcinoma. Moreover, overexpressing miR-940 induced G1 phase arrest; nevertheless, this effect could be counteracted by the overexpression of CD47 in lung adenocarcinoma cells. We further validated that miR-940 can directly modulate the activity of CD47.

We reviewed the literature and identified four regulatory pathways related to miR-940: the Wnt/β-catenin signaling pathway, the MAPK signaling pathway, the PD-1/PD-L1 checkpoint pathway, and the PI3K-Akt signaling pathway [18]. CD47 was found to promote the proliferation and migration of HEC-1A and Ishikawa cells and inhibit apoptosis by activating the PI3K/Akt/mTOR signaling pathway in endometrial cancer [7]. Similarly, another study on glioma confirmed that CD47 promotes glioma cell invasion by activating the PI3K/Akt pathway [8]. Our Western-blot experiments indicated that miR-940 can inhibit the PI3K-Akt signaling pathway, and downregulating CD47 expression yielded similar results. Also, the expression of p-AKT, p-PI3K, and p-mTOR proteins were lower, CD47 can attenuate the suppression effect of miR-940, further confirming that CD47 is a target of miR-940. This demonstrates that miR-940 inhibits CD47 expression through the PI3K-Akt signaling pathway, subsequently affecting the biological behavior of lung adenocarcinoma cells. Therefore, miR-940/CD47/PI3K-Akt represents a potential immunotherapy target, although additional studies are needed to explore whether downstream signaling pathways beyond PI3K-Akt have a synergistic regulatory effect.

In summary, our study uncovered the overexpression of CD47 in lung adenocarcinoma and provided evidence that miR-940 can impede the biological functions of lung adenocarcinoma cells by targeting CD47 through the PI3K/Akt signaling pathway. This research represents the inaugural documentation of the regulatory role of miR-940 on CD47 in non-small cell lung cancer (NSCLC), implying its promising potential as a target for clinical immunotherapy.

## Disclosure of conflict of interest

None.

**Address correspondence to:** Drs. Huawen Liu and Xiaoping Huang, Department of Oncology, Chongqing University Three Gorges Hospital, Chongqing University, No. 165 Xincheng Road, Wanzhou District, Chongqing 404100, China. E-mail: liuhw-008@163.com (H WL); huangxiaoping2020@cqu.edu.cn (XPH); Dr. Liping Fu, Department of Radiation Oncology, Shanghai East Hospital, Tongji University School of Medicine, No. 150 Jimo Road, Pudong District, Shanghai 200120, China. E-mail: flping2006@sina.com

## References

- [1] Siegel RL, Miller KD and Jemal A. Cancer statistics, 2019. *CA Cancer J Clin* 2019; 69: 7-34.
- [2] Puri S, Saltos A, Perez B, Le X and Gray JE. Locally advanced, unresectable non-small cell lung cancer. *Curr Oncol Rep* 2020; 22: 31.
- [3] Esfahani K, Roudaia L, Buhlaiga N, Del Rincon SV, Papneja N and Miller WH Jr. A review of cancer immunotherapy: from the past, to the present, to the future. *Curr Oncol* 2020; 27 Suppl 2: S87-S97.
- [4] Puri S, Shafique M and Gray JE. Immune checkpoint inhibitors in early-stage and locally advanced non-small cell lung cancer. *Curr Treat Options Oncol* 2018; 19: 39.
- [5] Herbst RS, Morgensztern D and Boshoff C. The biology and management of non-small cell lung cancer. *Nature* 2018; 553: 446-454.
- [6] Soto-Pantoja DR, Kaur S and Roberts DD. CD47 signaling pathways controlling cellular differentiation and responses to stress. *Crit Rev Biochem Mol Biol* 2015; 50: 212-230.
- [7] Liu Y, Chang Y, He X, Cai Y, Jiang H, Jia R and Leng J. CD47 enhances cell viability and migration ability but inhibits apoptosis in endometrial carcinoma cells via the PI3K/Akt/mTOR signaling pathway. *Front Oncol* 2020; 10: 1525.
- [8] Liu X, Wu X, Wang Y, Li Y, Chen X, Yang W and Jiang L. CD47 promotes human glioblastoma invasion through activation of the PI3K/Akt pathway. *Oncol Res* 2019; 27: 415-422.
- [9] Chao MP, Weissman IL and Majeti R. The CD47/SIRP $\alpha$  pathway in cancer immune evasion and potential therapeutic implications. *Curr Opin Immunol* 2012; 24: 225-232.
- [10] Jia X, Yan B, Tian X, Liu Q, Jin J, Shi J and Hou Y. CD47/SIRP $\alpha$  pathway mediates cancer immune escape and immunotherapy. *Int J Biol Sci* 2021; 17: 3281-3287.
- [11] Veillette A and Chen J. SIRP $\alpha$ -CD47 immune checkpoint blockade in anticancer therapy. *Trends Immunol* 2018; 39: 173-184.
- [12] Li X, Nie C, Tian B, Tan X, Han W, Wang J, Jin Y, Li Y, Guan X, Hong A and Chen X. miR-671-5p blocks the progression of human esophageal

## miR-940 suppress biological functions of lung adenocarcinoma cell

- squamous cell carcinoma by suppressing FGFR2. *Int J Biol Sci* 2019; 15: 1892-1904.
- [13] Zhu Z, Luo L, Xiang Q, Wang J, Liu Y, Deng Y and Zhao Z. MiRNA-671-5p promotes prostate cancer development and metastasis by targeting NFIA/CRYAB axis. *Cell Death Dis* 2020; 11: 949.
- [14] Xue J, Niu J, Wu J and Wu ZH. MicroRNAs in cancer therapeutic response: friend and foe. *World J Clin Oncol* 2014; 5: 730-43.
- [15] Tan X, Li Z, Ren S, Rezaei K, Pan Q, Goldstein AT, Macri CJ, Cao D, Brem RF and Fu SW. Dynamically decreased miR-671-5p expression is associated with oncogenic transformation and radiochemoresistance in breast cancer. *Breast Cancer Res* 2019; 21: 89.
- [16] Wang F, Wang Z, Gu X and Cui J. miR-940 up-regulation suppresses cell proliferation and induces apoptosis by targeting PKC-δ in ovarian cancer OVCAR3 cells. *Oncol Res* 2017; 25: 107-114.
- [17] Jiang K, Zhao T, Shen M, Zhang F, Duan S, Lei Z and Chen Y. MiR-940 inhibits TGF-β-induced epithelial-mesenchymal transition and cell invasion by targeting Snail in non-small cell lung cancer. *J Cancer* 2019; 10: 2735-2744.
- [18] Li H, Li Y, Tian D, Zhang J and Duan S. miR-940 is a new biomarker with tumor diagnostic and prognostic value. *Mol Ther Nucleic Acids* 2021; 25: 53-66.
- [19] Xu R, Zhou F, Yu T, Xu G, Zhang J, Wang Y, Zhao L and Liu N. MicroRNA-940 inhibits epithelial-mesenchymal transition of glioma cells via targeting ZEB2. *Am J Transl Res* 2019; 11: 7351-7363.
- [20] Luo H, Xu R, Chen B, Dong S, Zhou F, Yu T, Xu G, Zhang J, Wang Y and You Y. MicroRNA-940 inhibits glioma cells proliferation and cell cycle progression by targeting CKS1. *Am J Transl Res* 2019; 11: 4851-4865.
- [21] Hayat SMG, Bianconi V, Pirro M, Jaafari MR, Hatamipour M and Sahebkar A. CD47: role in the immune system and application to cancer therapy. *Cell Oncol (Dordr)* 2020; 43: 19-30.
- [22] Feng M, Jiang W, Kim BYS, Zhang CC, Fu YX and Weissman IL. Phagocytosis checkpoints as new targets for cancer immunotherapy. *Nat Rev Cancer* 2019; 19: 568-586.
- [23] Feng R, Zhao H, Xu J and Shen C. CD47: the next checkpoint target for cancer immunotherapy. *Crit Rev Oncol Hematol* 2020; 152: 103014.
- [24] Xu Y, Li J, Tong B, Chen M, Liu X, Zhong W, Zhao J and Wang M. Positive tumour CD47 expression is an independent prognostic factor for recurrence in resected non-small cell lung cancer. *ESMO Open* 2020; 5: e000823.
- [25] Shi M, Gu Y, Jin K, Fang H, Chen Y, Cao Y, Liu X, Lv K, He X, Lin C, Liu H, Li H, He H, Qin J, Li R, Zhang H and Zhang W. CD47 expression in gastric cancer clinical correlates and association with macrophage infiltration. *Cancer Immunol Immunother* 2021; 70: 1831-1840.

## miR-940 suppress biological functions of lung adenocarcinoma cell

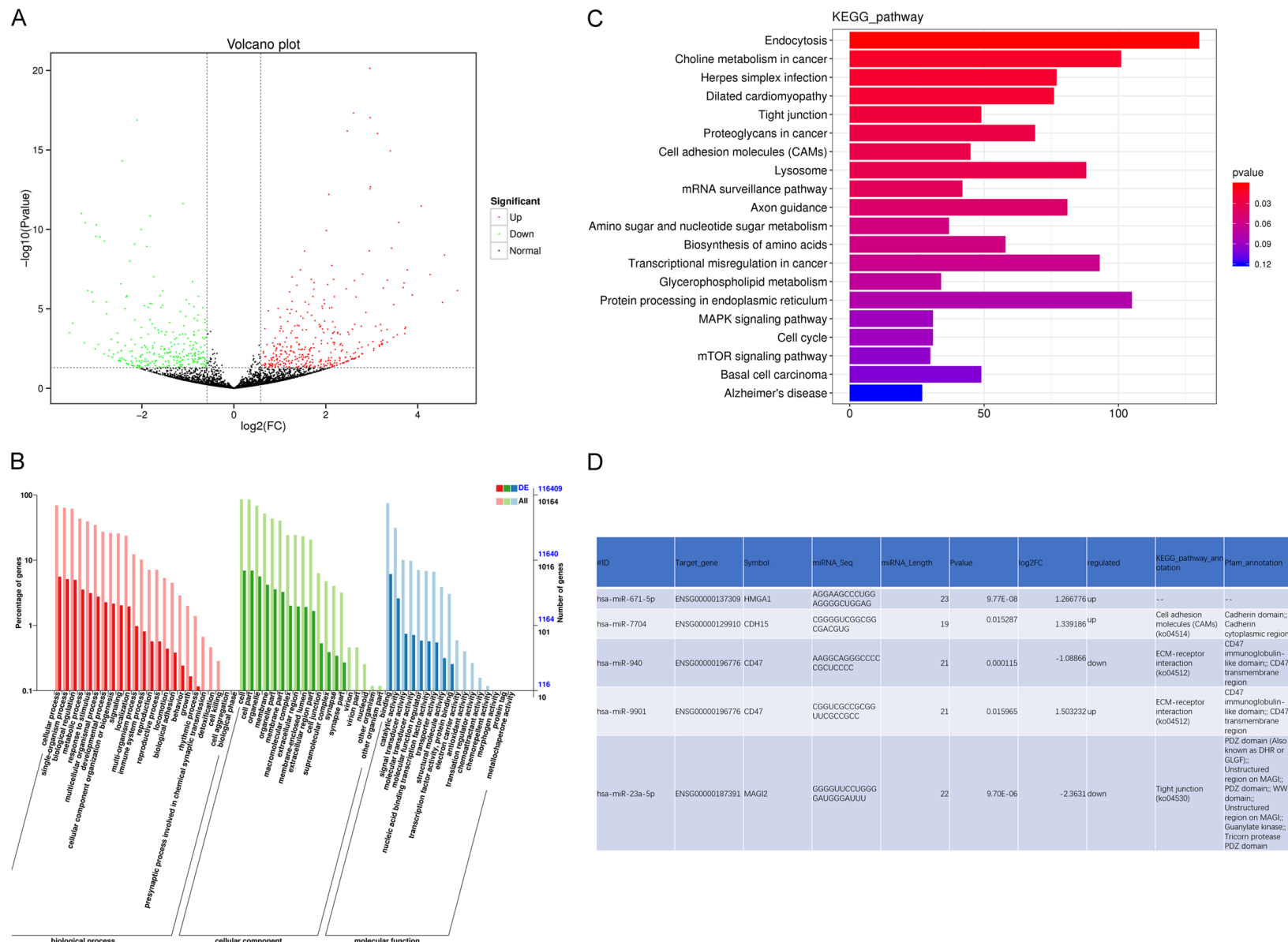


**Figure S1.** Differential expression of miRNAs between NSCLC tissues and normal controls. A. Volcano plot showing the differential miRNAs in NSCLC tissues and normal tissues. B. Gene ontology analysis showing the enrichment scores of GO terms such as BP, CC, and MF. C. KEGG pathway analysis indicating the enrichment of differential miRNA target genes. D. The candidate gene in the tissues.